pp. 1–14 (2014)

Hybrid cellular automaton method for homogeneous tumour growth modelling

K. M. Zapolski*, Yu. B. Admiralskiy*, and A. S. Bratus*†

Abstract — In this paper a discrete planar model of the tumour growth is presented. The model is based on hybrid cellular automaton and describes the tumour in a homogeneous tissue. The tissue consists of healthy cells and can have irregular vasculature. The model simulates proliferation processes and necrotic cells appearance which depends on the oxygen supply. There exists a stable solution, which may be used as an approximation of the tissue. Described HCA model can be extended with angiogenesis, nutrients and factors fields.

Keywords: Hybrid cellular automaton, tumour proliferation, tumour modelling, cancer modelling.

1. Introduction

Cancer is one of the most common reasons of death in many countries of the world. It is the case, because tumour is a very inconvenient object to detect and cure. Today it is hard to detect tumour while it is small. Modern tests for tumour markers may help find cancer in healthy or high-risk people before symptoms develop, however the presence of the marker alone is not enough to diagnose cancer. Another problem lies in types of cancer treatment. Chemo or radiation therapies cause healthy cells death and need to be used with care. That's why we need good tumour models which can predict tumour reaction to treatment and help find out new signs of cancer presence.

The most essential property of cancer tumour is its fast growth. Methods of tumour growth modelling often use continuous dynamic models. Despite undoubted progress in that area, many mathematical and modelling problems remain. Difficulties with continuous models make researchers look for other modelling methods. For example discrete models, which are based upon cellular automata, are widely used.

The article is dedicated to the tumour growth model which is based upon the hybrid cellular automata (HCA) approach. The model describes the tumour growth dependence on the oxygen supply. In the first part the HCA construction method is described. It combines the discretized classical diffusion equation with cellular automaton. Such an approach helps us to avoid a postulation of oxygen field rules

*Moscow State University, Faculty of Computational Mathematics and Cybernetics.

†Corresponding author. E-mail: alexander.bratus@yandex.ru

and shows the role of cellular automaton in the model. In the second part some model simulation results are given. They describe the typical behaviour of obtained solutions.

1.1. Existing models review

The cancer modelling has a long history. There are many cancer modelling approaches, which are based on different mathematical methods (see [9, 15]). This paper is dedicated to the tumour growth modelling. There are many types of tumours and each type has its own properties. Some papers are devoted to the solid tumour modelling (see [3]). We can also find articles which describe general aspects of tumour growth (see [6]). In the following sections we give a short review of such models.

1.1.1. Continuous tumour growth models. Today the most part of continuous tumour growth models can be separated into two classes: the lumped element model and the distributed element model.

In practice researchers use the lumped element models when they are interested in tumour cells count or other tumour integral characteristics. In such models the whole tumour is considered as a single object. It is useful to describe tumour response to the treatment (chemotherapy and etc.). However such models do not describe the distribution of tumour in space or shape. In these models the dynamics of tumour growth is described by ordinary differential equations (ODEs) system with tumour parameters as variables. It provides us with good analytical methods to predict the system evolution. One of the system variables is often a cell count, but in some papers different cell classes are marked out. For example in [13] all the cells were separated into two classes according to their cell-cycle states.

The other way to describe tumour is the distributed element model. The parameters of tumour (density for example) are distributed continuously throughout space. It provides the way to describe the behaviour of separate parts of tumour. This model can give a proper account to distribution and uptake of oxygen, nutrients and production of carbon dioxide in tumour. However it is hard to describe some tumour characteristics with such models (for example, the solid tumour borders), because they operate with partial differential equations (PDEs). The distributed element model of infiltrative tumour is used in [12] to obtain growth rate dependence on oxygen amount. In [2] such a model is used to describe the cancer cell invasion of healthy tissue.

There are also papers where a hybrid model is used. Such a combination of continuous lumped and distributed element models can help describe drug delivery processes (see [7]).

1.1.2. Discrete models. On the one hand ODE systems are unable to describe tumour spatial structure. On the other hand PDE systems don't provide any intuitive way to describe some tumour growth aspects. For example in [5] the multicellular

spheroids growth is described by using a free boundary-value problem. Nowadays such problems need serious simplifications to be analyzed. These disadvantages of continuous models make researchers propose other models of tumour proliferation.

Many papers are devoted to discrete models. In [10] the cellular automaton for proliferation modelling was used. In [1] the influence of oxygen concentration to the cell colony growth was described by using hybrid cellular automaton. In our work we describe the construction and solutions behaviour of similar model with irregular vascular network.

1.2. Hybrid cellular automaton

The cellular automaton is an idealized model of physical system with discrete space and time. The base of the model is the square grid of elements which are called cells. Each cell has its own coordinates $\bar{r}$ and cell state S. The state can represent any characteristic of the cell, but the set of all the states $\mathscr{S}$ must be a finite set. Each cell has the neighbourhood set which consists of the cells with coordinates $\bar{r}$ in the grid:

$$\mathscr{N}(\bar{r}) = \{\bar{r} + \Delta_i \,|\, i = 1, \ldots, N\}.$$

Over time, changes in cell states put together the evolution of the whole system (in our paper we consider only synchronous CA):

$$S_n(\bar{r}) = R\left(S_{n-1}(\bar{r}), S_{n-1}(\mathscr{N}(\bar{r}))\right).$$

In the case of the finite grid we need to define how to process the boundary cells. Boundary cells processing rules are called boundary conditions.

The cellular dynamics in real tissue depends on many factors: nutrient and toxin amount, temperature. etc. We can consider these factors as fields. The field itself can be modeled with asynchronous CA (see [4]). But in our research the other way — hybrid cellular automaton (HCA) is used. The HCA is a model where the classical CA is combined with some field (which is not modeled by CA). This extension of the classical automaton provides the ability to consider the global characteristics of the problem. The HCA basics and some applications are described in [16].

Assume that the state of the cell can be presented as the vector $[S_{D_1}, S_{D_2} \ldots, S_{D_N}]^T$. The hybrid automaton cell will have the state:

$$S = [S_{D_1}, \ldots, S_{D_N}, S_{F_1}, \ldots, S_{F_M}]^T.$$

Vector components $S_{D_1}, \ldots, S_{D_N}$ are the design variables, components $S_{F_1}, \ldots, S_{F_M}$ are the field variables. The field influences the local transition rules of cellular automaton and may change over time.

2. Model description

We consider a 2D model for visualization purposes, but there are no principal limitations that prevent us from generalizing it for the 3D space. The model is kept simple

in order to make the description of mathematical aspects of construction clear. It doesn't consider angiogenesis, tumour invasion or immune system reaction.

In the model we consider small tumours which contains several hundred up to several tens of thousands of cells ($\approx 5\,\mathrm{mm}^2$). In that scale we assume the tumour and surrounding tissue to be homogeneous, where cells put together a regular structure (so the cell density changes insignificantly) and have similar characteristics (size, oxygen uptake rate and etc.). These conditions provide an ability to represent tissue cells and capillaries by CA elements in square lattice. Capillaries supply tissue and tumour cells with oxygen and can form an irregular network. We concentrate on the aerobic respiration, so model describes tumour cells dynamics dependence only on oxygen extraction and uptake. Respiration is the main energy source for cells which are located near capillaries.

We consider a rectangular region of tissue (or extracellular matrix) with a tumour inside it. All cells are contained in rectangular domain D. The origin of coordinates is in left-down vertex of rectangle. Each point of the rectangle D has coordinates $\bar{x} = [x_1, x_2]^T \geqslant 0$.

2.1. Periodical functions

To describe the field discretization properties we need to define fluctuation functions.

Definition 2.1. Function $\varphi(\bar{x})$, where $\bar{x} \in \mathbb{R}^n$ is the *fluctuation function* if it fulfills two conditions:

(1) has limitation: $|\varphi(\bar{x})| < C$ for all $\bar{x} \in \mathbb{R}^n$;

(1) has compact support B: $\varphi(\bar{x}) = 0$ for all $\bar{x} \notin B \subset \mathbb{R}^n$.

If B is a convex compact and $\bar{0} \in B$ we can define a periodical fluctuation. Let us consider $\bar{r}_0 \in \mathbb{R}^n$ and $R \in \mathbb{R}^{n\times n}$. The $\bar{r}_0$ and R must fulfill the condition:

$$R = \begin{bmatrix} \vdots & \dots & \vdots \\ \bar{r}_1, & \dots, & \bar{r}_n \\ \vdots & \dots & \vdots \end{bmatrix}, \quad \bar{r}_1, \dots, \bar{r}_n \text{ — basis vectors}$$

$$\bar{r}_0 = c_1 r_1 + \dots + c_n r_n, \quad |c_i| < 1, \quad i = 1, \dots, n.$$

In the area D we consider the subset of vectors:

$$K[\bar{r}_0, R, D] = \left\{ [k_1, \dots, k_n]^T \in \mathbb{Z}^n \,\middle|\, \bar{r}_0 + \sum_{i=1}^{n} k_i \bar{r}_i \in D \right\}.$$

Area D is a limited set, so $|K[\bar{r}_0, R, D]| = N_K < +\infty$. For all the pairs $\tilde{r}_1 = \bar{r}_0 + \sum_{i=1}^{n} k_{1i} r_i$ and $\tilde{r}_2 = \bar{r}_0 + \sum_{i=1}^{n} k_{2i} r_i$, where $\tilde{r}_1 \neq \tilde{r}_2$ and $k_1, k_2 \in K[\bar{r}_0, R, B]$, there

exists $r > 0$ which fulfills the condition:

$$\|\tilde{r}_1 - \tilde{r}_2\| = \left\| \sum_{i=1}^{n} (k_{1i} - k_{2i})\, \bar{x}_i \right\| > 2r.$$

We also demand the matrix R to fulfill the condition:

$$r > r_b = \max_{x \in B} \|x\|.$$

In Minkowski addition notation it means:

$$(\tilde{r}_1 + B) \cap (\tilde{r}_2 + B) = \varnothing.$$

For these objects r_0, R, B, $\varphi(\bar{x})$ the following function can be defined on area D:

$$\tilde{\varphi}\left[\bar{r}_0, R, B\right](\bar{x}) = \begin{cases} \varphi(\bar{x} - \tilde{r}), & x \in (\tilde{r} + B) \\ \tilde{r} = \bar{r}_0 + \sum\limits_{i=1}^{n} k_i \bar{r}_i, & [k_1, \ldots, k_n]^T \in K\left[\bar{r}_0, R, B\right] \\ 0, & \text{otherwise.} \end{cases}$$

For each fluctuation function specified on compact B the following operator can be defined:

$$\tilde{\cdot}\left[\bar{r}_0, R, B\right] : \varphi(\cdot) \to \tilde{\varphi}\left[\bar{r}_0, R, B\right](\cdot).$$

The interpretation of $\tilde{\varphi}\left[\bar{r}_0, R, B\right](\cdot)$ is quite simple: with every vector $k \in K\left[\bar{r}_0, R, B\right]$ the location $\tilde{r} = \bar{r}_0 + \sum_{i=1}^{n} k_i \bar{r}_i$ can be associated, and $\tilde{\varphi}\left[\bar{r}_0, R, B\right](\cdot)$ equals to the value of $\varphi(\bar{x})$ if the $\tilde{r}$ is the origin of coordinates (we remember that $\bar{0} \in B$). The function has support which is a subset of a ball with center $\bar{0}$ and radius r. Supports for two different locations do not intersect, and that's why the function $\tilde{\varphi}\left[\bar{r}_0, R, B\right](\cdot)$ is determined explicitly.

Let us enumerate all the elements:

$$K\left[\bar{r}_0, R, D\right] = \left\{\bar{k}_1, \ldots, \bar{k}_{N_K}\right\}$$

and consider a function:

$$\bar{C}(\bar{x}, \bar{y}) \;=\; \left[C_1(\bar{x}, \bar{y}), \ldots, C_{N_K}(\bar{x}, \bar{y})\right]^T \;\in\; \mathbb{R}^N, \quad \bar{x} \in B.$$

Here $\bar{y}$ are parameters. So the following operation can be defined:

$$\bar{C}(\bar{x}, \bar{y}) \cdot \tilde{\varphi}\left[\bar{r}_0, R, B\right](\bar{x}) = \begin{cases} C_i(\bar{x} - \tilde{r}_i, \bar{y})\varphi(\bar{x} - \tilde{r}_i), & x \in (\tilde{r}_i + B) \\ \tilde{r}_i = \bar{r}_0 + \sum\limits_{j=1}^{n} k_{ij} \bar{r}_j, & \bar{k}_i = [k_{i1}, \ldots, k_{in}]^T \in K\left[\bar{r}_0, R, D\right] \\ 0, & \text{otherwise.} \end{cases}$$

The example of fluctuation function $\varphi(x, y)$ is shown in Fig. 1 (the border of the set B is shown as a red line). The result of $\tilde{\varphi}[\bar{r}_0, R, B](x, y)$ is shown in Fig. 2, where

$$D = (0, 10) \times (0, 10), \quad B = \left\{(x, y) \,\middle|\, x^2 + y^2 \leqslant 1\right\}$$

$$\bar{r}_0 = [1, 1]^T, \quad R = \begin{bmatrix} 4 & 0 \\ 0 & 4 \end{bmatrix}.$$

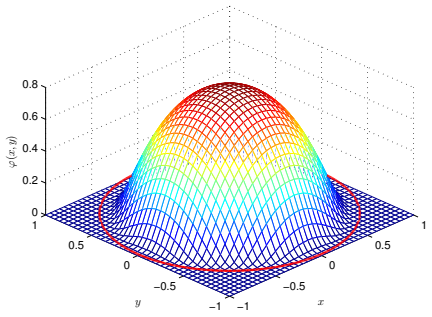

Figure 1. Fluctuation function in $\mathbb{R}^2$.

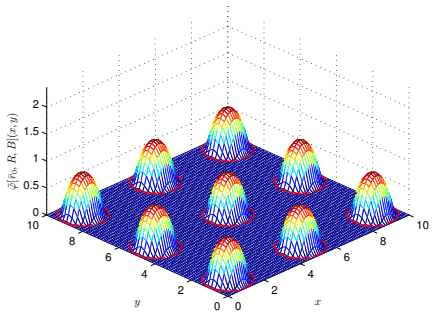

Figure 2. Periodical fluctuation function in $\mathbb{R}^2$.

2.2. Oxygen field

The oxygen concentration $u(\bar{x},t)$ is defined on the set $\bar{D}\times[t_0,T]$. Oxygen is extracted by capillaries and is consumed by cells. The oxygen field behaviour can be described by the diffusion equation:

$$\frac{\partial u}{\partial t} = \nabla\left(F(\bar{x},t)\nabla u\right) + E(\bar{x},t), \quad \bar{x}\in D, \quad t\in(t_0,T]. \tag{2.1}$$

Boundary conditions are:

$$\begin{cases} u(\bar{x},t_0) = u_0(\bar{x}), & \bar{x}\in\bar{D} \\ \dfrac{\partial u}{\partial \bar{n}}(\bar{x},t)\Big|_{\bar{x}\in\partial D} = a(\bar{x})|_{\bar{x}\in\partial D}, & t\in[t_0,T]. \end{cases}$$

Here $E(\bar{x},t)$ and $F(\bar{x},t)$ are continuous on $\bar{D}$ at every $t\in[t_0,T]$ and piecewise continuous function on $[t_0,T]$ with a finite number of singularities (so it has a piecewise smooth solution); $u_0(\bar{x})$ is continuous on $\bar{D}$; $a(\bar{x})$ is continuous on ∂D. The equation (2.1) is a very rough approximation of real oxygen field. However similar oxygen field models are used to obtain values from experimental data in some papers (for example in [8]). The equation is linear, that's why $E(\bar{x},t)$ (and the solution also) is able to be negative. Because of that we can't use it in PDE based continuous model. But we will show how the CA presence changes the situation.

First of all the classical partial differential equation describes the field, which is continuous over time and space. However, the CA is discrete, so we need to discretize the equation. Let us consider a rectangular domain D which has width L_{x_1} and height L_{x_2}. We also assume that there exist numbers $K, M\in\mathbb{N}$ for which:

$$\frac{L_{x_1}}{K} = \frac{L_{x_2}}{M} = \Delta x.$$

We can separate D into $N = KM$ square subareas D_{ij} according to the rule:

$$D_{ij} = \left\{ [x_1,x_2]^T \,\middle|\, x_1\in((i-1)\Delta x, i\Delta x),\ x_2\in((j-1)\Delta x, j\Delta x) \right\}.$$

For each area D_{ij} there is a unique corresponding CA element $S_{ij} \in \mathscr{S}$. Assume that CA transits into the following state at the moments:

$$t_0 + \Delta t, t_0 + 2\Delta t, \ldots, t_0 + Z\Delta t, \quad \Delta t = \frac{T - t_0}{Z}, \quad Z \in \mathbb{N}.$$

Coefficients in (2.1) will have singularities at these transition points. Cellular automaton has $N = KM$ cells and it passes $Z+1$ states on segment $[t_0, T]$.

Fluctuation functions can describe heterogeneity of oxygen diffusion and extraction (uptake) rate inside the cell. The homogeneity of tissue means that fluctuation functions are the same for all the cells. We consider convex compact $B \in \mathbb{R}^2$ which fulfills the following conditions:

(1) $\bar{0} \in B$;

(2) limitation condition: $B \subset \left(-\frac{\Delta x}{2}, \frac{\Delta x}{2}\right) \times \left(-\frac{\Delta x}{2}, \frac{\Delta x}{2}\right)$.

In that case set B has the following property:

$$B - \left[\frac{\Delta x}{2}, \frac{\Delta x}{2}\right]^T + [i\Delta x,\, j\Delta x]^T \subset D_{ij}. \tag{2.2}$$

Cells consume and extract oxygen and may have variable diffusion coefficient. To describe these characteristics we define in B continuous fluctuation functions $\psi(\bar{x})$ and $\varphi(\bar{x})$. For $\varphi(\bar{x})$ there are additional conditions:

(1) non-negativity: $\varphi(\bar{x}) \geqslant 0$, where $\bar{x} \in B$;

(2) has an integral: $\int_B \varphi(\xi)\, \mathrm{d}\xi = 1$.

By using the operation defined in Subsection 2.1, we can rewrite (2.1) more exactly:

$$\frac{\partial u}{\partial t} = \nabla\left((F_0 + \bar{F}(t) \cdot \tilde{\psi}[\bar{r}_0, R, B](\bar{x}))\, \nabla u\right) + \bar{C}(t) \cdot \tilde{\varphi}[\bar{r}_0, R, B](\bar{x}) \tag{2.3}$$

where $\bar{C}(t)$ and $\bar{F}(t)$ are piecewise constant and:

$$F_0 + \bar{F}(t) \cdot \tilde{\psi}[\bar{r}_0, R, B](\bar{x}) > 0, \quad (\bar{x}, t) \in D \times [t_0, T]$$

$$\bar{r}_0 = \left[\frac{\Delta x}{2}, \frac{\Delta x}{2}\right]^T; \quad R = \begin{bmatrix} \Delta x & 0 \\ 0 & \Delta x \end{bmatrix}.$$

Now we can mathematically express what the 'homogeneity' of tissue in the model means:

(1) tissue cells put together a rectangular lattice. So it's possible to separate area D into a set of regions D_{ij}, and there is a unique cell which is located in each region;

(2) the oxygen field equation inside the tissue can be described in the form (2.3).

2.2.1. Field discretization. The equation (2.3) can be discretized. We assume that $u(x,t)$ is a solution of (2.3).

(1) Instead of $u(\bar{x},t)$ we consider new variables $Q_{ij}(t)$:

$$Q_{ij}(t) = \int\limits_{D_{ij}} u(\xi,t)\,\mathrm{d}\xi.$$

Variable $Q_{ij}(t)$ can be interpreted as an amount of oxygen inside D_{ij} at the moment t.

(2) We integrate equation(2.3) on area D_{ij} and use Kelvin–Stokes theorem:

$$\int\limits_{D_{ij}} \frac{\partial u}{\partial t}(\xi,t)\,\mathrm{d}\xi = F_0 \int\limits_{\partial D_{ij}} \langle \nabla u, n\rangle(\xi,t)\,\mathrm{d}\xi + F_{ij}(t) \int\limits_{\partial D_{ij}} \langle \tilde{\psi}[\bar{r}_0,R,B]\nabla u, n\rangle(\xi,t)\,\mathrm{d}\xi + C_{ij}(t).$$

According to the area B property (2.2) and Definition 2.1:

$$\tilde{\psi}[\bar{r}_0,R,B](\bar{x})|_{\bar{x}\in\partial D_{ij}} = 0.$$

(3) For every $i = 1,\ldots,K$ and $j = 1\ldots,M$ we approximate $Q_{ij}(t)$ time derivative with its difference analogue:

$$\frac{Q_{ij}^k - Q_{ij}^{k-1}}{\Delta t} = F_0 \sum_{r=0}^{1} (-1)^r \left(q^{x_1}_{(i-r)j}(k-1) + q^{x_2}_{i(j-r)}(k-1) \right) + C_{ij}^{k-1}, \quad k = 1,\ldots,Z.$$

For every $k = 0,\ldots,Z-1$ boundary $q^{x_1}_{ij}(k)$ and initial Q^0_{ij} values are:

$$q^{x_1}_{0j}(k) = -\int\limits_{(j-1)\Delta x}^{j\Delta x} a(0,\xi)\,\mathrm{d}\xi, \quad q^{x_1}_{Kj}(k) = \int\limits_{(j-1)\Delta x}^{j\Delta x} a(L_{x_1},\xi)\,\mathrm{d}\xi, \quad Q^0_{ij} = \int\limits_{D_{ij}} u_0(\xi)\,\mathrm{d}\xi.$$

Boundary $q^{x_2}_{ij}(k)$ can be obtained from the same type formulas as $q^{x_1}_{ij}(k)$. Internal $q^{x_1}_{ij}(k)$ and $q^{x_2}_{ij}(k)$ values are:

$$q^{x_1}_{ij}(k)\Delta x^2 = Q^k_{(i+1)j} - Q^k_{ij}, \quad q^{x_2}_{ij}(k)\Delta x^2 = Q^k_{i(j+1)} - Q^k_{ij}$$
$$i = 1,\ldots,K-1, \quad j = 1\ldots,M-1.$$

The discretized equation has less parameters count. Variables Q^k_{ij} are model HCA field variables and CA works with discretized Q^k_{ij} field.

2.3. Cell states

Elements of cellular automaton represent regions with biological cells (normal, cancer cells) and capillaries. Each subarea D_{ij} contains only one cell. To process boundary cells we use adiabatic boundary conditions. In the model the following types of cells are marked out:

(1) empty cell — region is outside of the tissue area or filled with extracellular matrix;

(2) normal and cancer cells — tissue and tumour cells;

(3) capillary.

Cells of the same type have similar characteristics and state transitions. For normal tissue and cancer cells we simulate the cell cycle:

(1) specialized state (G_0) — normal oxygen uptake, no doubling (Gap 0);

(2) doubling (D) — the state which includes preparation (Gap 1), DNA replication (S), preparations for mitosis (Gap 2) and mitosis (M). The cell consumes more oxygen than in G_0 state;

(3) hypoxia (H) — cell's oxygen supply is insufficient for a normal activity. If the oxygen amount remains insufficient, the cell reaches necrosis N state;

(4) necrosis (N) — no oxygen uptake, the cell is dead. Dead cells are removed after time T_N.

The cancer cell has a similar cycle, but reaches the G_0 state only if there is no space to proliferate. The cell proliferates if the oxygen supply is enough and some neighbour position is empty. The transition between states is made according to the cell cycle. Sufficient oxygen supply is required to remain in G_0 and D states. Otherwise the cell reaches the hypoxia (H) and then necrosis N states (it provides the non-negativity of Q_{ij}^k solution). If the sufficient supply of oxygen is restored, the cell reaches a specialized state G_0.

Capillaries have only one state — the extraction state, in which the capillary extracts oxygen to supply surrounding tissue. A vessel can be approximated as a connected group of capillary cells. Let us define the sets:

$S_{\text{type}} = \{\text{Empty}, \text{Normal}, \text{Cancer}, \text{Capillary}\}$ — the cell types set;

$S_{\text{int}} = \{G_0, D, H, N\}$ — the internal states set;

$\tilde{T} = \{1, \ldots, T_{\text{lim}}\}$ — the number of iterations the cell has remained in the state (maximum T_{lim}).

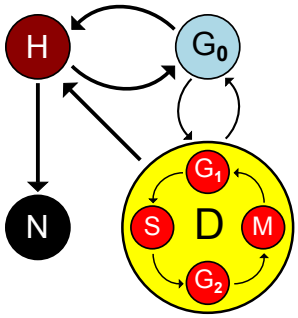

Figure 3. Simplified cell cycle. Doubling stages united into *D* state.

By using this definition we can determine the cellular automaton cell states set. Each state can be presented as:

$$S = [S_t, S_i, t] \in \mathscr{S}, \quad S_t \in S_{\text{type}}, S_i \in S_{\text{int}}, t \in \tilde{T}$$
$$\mathscr{S} = S_{\text{type}} \times S_{\text{int}} \times \tilde{T}.$$

The S components are the design variables of HCA.

2.4. Field and CA

The cellular automaton dynamics can be written as:

$$S_i^k = R(S_i^{k-1}, S^{k-1}(\mathscr{N}_i)), \quad k = 1, \ldots, Z$$
$$S_i^0 \in \mathscr{S}.$$

The CA remains in k-th state for a period of time:

$$S_i(t) = S_i^k, \quad t \in [t_0 + k\Delta t, t_0 + (k+1)\Delta t).$$

The CA interacts with field by changing multipliers $\bar{C}(t)$ and $\bar{F}(t)$ in equation (2.3). We consider that two cells in the same state interact with the oxygen field in the same manner:

$$\begin{aligned} \bar{C}(t) &= C(S(t)) = [C(S_1(t)), \ldots, C(S_N(t))] \in \mathbb{R}^N \\ \bar{F}(t) &= D(S(t)) = [F(S_1(t)), \ldots, F(S_N(t))] \in \mathbb{R}^N. \end{aligned} \tag{2.4}$$

The HCA gives to the model several advantages. Different cell types mark out the borders between tumour and surrounding tissue. The CA can be extended with angiogenesis (capillaries take part in cell dynamics). These factors provide a way to avoid a free boundary-value problem (like in [5]). The automaton switches constants $\bar{C}(t)$ and $\bar{F}(t)$ and keeps the field solution Q_{ij}^k non-negative. The HCA states can be calculated in parallel manner because the state of each cell at the next moment depends on cells only in the neighbourhood set.

Table 1. Function $C(S)$.

$S_t \backslash S_i$	G_0	D	H	N
Normal	$-C_0^n$	$-C_D^n$	0	0
Cancer	$-C_0^c$	$-C_D^c$	0	0

Table 2. Parameters values.

Parameter	Value	Description
Δx	$50\,\mu$m	Averange cell size
Δt	0.5 s	Time step (assumed)
F_0	$2\times10^3\ \mu\text{m}^2/\text{s}$	Oxygen diffusivity in thin cell layer [8]
C_P	$4.7\ \text{nmol}/\text{s}/10^6$	Capillary oxygen extraction rate (assumed)
C_0^n	$0.4\ \text{nmol}/\text{s}/10^6$	Normal cell OUR in G_0 [11]
C_D^c	$0.7\ \text{nmol}/\text{s}/10^6$	Cancer cell OUR in D [14]
T_D^n	60.1×10^3 s	Normal cell doubling time
T_D^c	71.3×10^3 s	Cancer cell doubling time
T_N	10.8×10^3 s	Necrosis time (assumed)

3. Discussion and modelling results

In fact we can use in each D_{ij} its own fluctuation functions $\varphi(\bar{x})$ and $\psi(\bar{x})$, but they must fulfill the described conditions (see Subsection 2.2). The discretized model is simpler and has less parameters count than the continuous one. Function $C(S)$ in equilibrium (2.4) is always 0 for empty cells and C_P for capillaries. For normal and cancer cells the function is shown in Table 1. We assume $a(\bar{x}) = 0$ in ∂D. There are constants which need to be estimated: cell doubling oxygen uptake rate (OUR) of normal (C_D^n) and cancer (C_D^c), cell G_0 OUR for normal (C_0^n) and cancer cell (C_0^c), G_0 duration for normal cells (T_0^n), time limit for hypoxic normal (T_h^n) and cancer (T_h^c) cells. We assume that constants are:

$$C_D^n = \frac{3}{2}C_0^n, \quad C_D^c = \frac{3}{2}C_0^c, \quad T_0^n = \frac{1}{2}T_D^n, \quad T_h^n = T_h^c = \frac{1}{2}T_0^n.$$

In our simulations we use parameters values for thin cell layers obtained by the experiments. Normal cells represent hepatocytes (normal Chang liver cell line) and cancer cells represent HepG2 (hepatocellular carcinoma) cells. Used values are shown in Table 2.

At first the tumour growth dependence on capillaries count on the 20×20 field (1 mm^2) was investigated. The tumour had started with one cell and had been proliferating for two weeks (336 hours). During the proliferation an oxygen amount $Q^k = \sum_{i=1}^{K}\sum_{j=1}^{M} Q_{ij}^k$ and a cancer cells count were being obtained. There are two scenarios of the HCA dynamics: infinite oxygen and stable scenarios (Fig. 4). First one takes place when capillaries oxygen extractions exceed the whole possible field consumption (37 capillary cells). Tumour had occupied all free cells and then stopped growing (Fig. 5). In the second scenario we used 12 capillary cells (see Fig. 7), what is not enough to supply the large tumour with oxygen. The growing

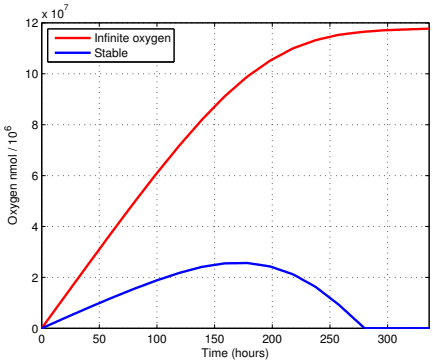

Figure 4. Oxygen amount Q^k.

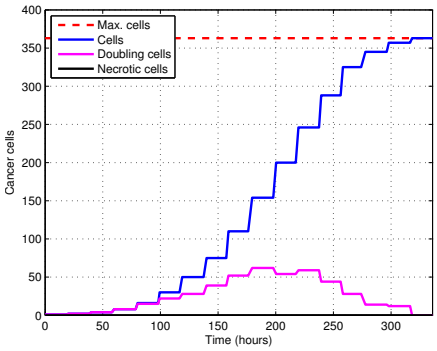

Figure 5. Infinite oxygen scenario.

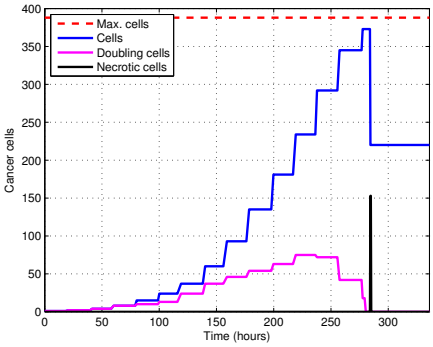

Figure 6. Stable scenario.

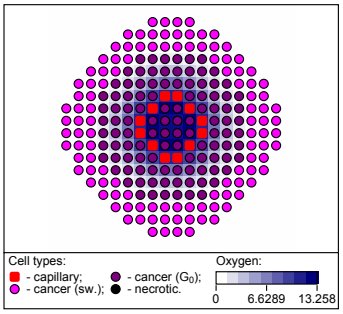

Figure 7. Stable tumour. Bright cells switch between G_0 and H states.

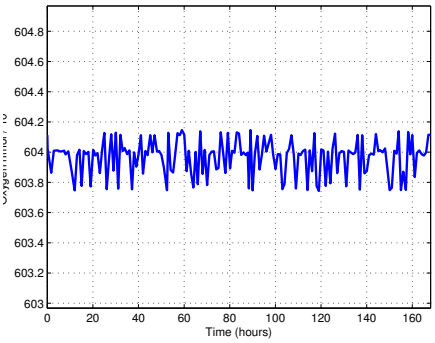

Figure 8. Stable tumour oxygen.

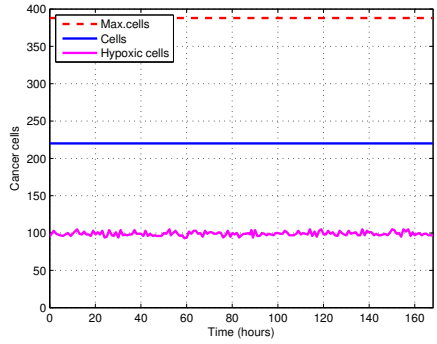

Figure 9. Stable tumour cells count.

tumour had consumed all extra oxygen and then decreased in size after 286 hours (Fig. 6). At this moment a necrotic border (or a core, if the tumour is surrounded by capillaries) appears. It corresponds with known fluorescence images of the solid tumour microenvironment. Since that moment there is no proliferation — tumour has been stabilized. In fact that's the start point when the angiogenesis is necessary for the further growth.

We also simulated stable tumour (Fig. 7) dynamics for a week (168 hours). The stable solution may also be characterized by several boundary cells, which are switching between hypoxia and specialized state (Fig. 7). The oxygen dynamics is shown in Fig. 8 (averange: 603.97 nmol$/10^6$, $\sigma = 0.11$ nmol$/10^6$). The cell dynamics is shown in Fig. 9 (averange: 99.08 hypoxic cells, $\sigma = 2.84$ cells). No switching cell in Fig. 7 remains in hypoxia H state for a long time, but the instantaneous H cells count varies insignificantly.

There is no cell invasion in the current model, so normal and cancer tissue invades only empty cells. Cancer cells always proliferate in the case of enough space and oxygen around. That's why they surpass normal cells, which passes also G_0 state.

4. Conclusion

The model is simple and doesn't simulate many important processes in real tumours. However the useful feature of the HCA approach was described: nonlinearity can be 'split' between field and CA to keep each of the components simple and intuitive. Also a 3D HCA model can be created with the described construction method. Stable solutions can be used as an approximation of real biological tissue, where oxygen uptake and extraction are balanced. Such a solution can be taken as an initial condition for more advanced model. The model can be extended to describe angiogenesis and other phenomena by adding extra fields and CA rules.

References

1. T. Alarcon, H. M. Byrne, and P. K. Maini, Towards whole-organ modelling of tumour growth. *Progress Biophys. Molecular Biology* **85-2,3** (2004), 451-472.
2. V. Andasari, A. Gerisch, G. Lolas, A. P. South, and M. A. J. Chaplain, Mathematical modelling of cancer cell invasion of tissue: biological insight from mathematical analysis and computational simulation. *J. Math. Biology* **63-1** (2011), 141–171.
3. R. P. Araujo and D. L. S. McElwain, A history of the study of solid tumour growth: The contribution of mathematical modelling. *Bulletin Math. Biology* **66-5** (2004), 1039–1091.
4. O. Bandman, Discrete models of physicochemical processes and their parallel implementation. *Lecture Notes in Computer Science* **6083** (2010), 20–29.
5. H. M. Byrne and M. A. J. Chaplain, Free boundary value problems associated with the growth and development of multicellular spheroids. *European J. Appl. Math.* **8-6** (1997), 639–658.
6. V. Cristini and J. S. Lowengrub, *Multiscale Modelling of Cancer: An Integrated Experimental and Mathematical Modelling Approach*. Cambridge University Press, Cambridge, 2010.

7. S. Eikenberry, A tumour cord model for Doxorubicin delivery and dose optimization in solid tumours. *Theor. Biology Medical Modelling* **6-1** (2009), 1–20.

8. D. R. Grimes, C. Kelly, K. Bloch, and M. Partridge, A method for estimating the oxygen consumption rate in multicellular tumour spheroids. *J. Royal Soc. Interface* **11–92** (2014), 2013–1124.

9. P. J. Gutiérrez Diez, I. H. Russo, and J. Russo *The Evolution of the Use of Mathematics in Cancer Research*. Springer, New York, 2012.

10. A. R. Kansal, S. Torquato, G. R. Harsh IV, E. A. Chiocca, and T. S. Deisboeck, Simulated brain tumour growth dynamics using a three-dimensional cellular automaton. *J. Theor. Biology* **203-4** (2000), 367–382.

11. S. Kidambi, R. S. Yarmush, E. Novik, P. Chao, M. L. Yarmush, and Y. Nahmias, Oxygen-mediated enhancement of primary hepatocyte metabolism, functional polarization, gene expression, and drug clearance. *Proc. National Academy Sci.* **106-37** (2009), 15714–15719.

12. A. V. Kolobov, V. V. Gubernov, and A. A. Polezhaev, Autowaves in the model of inflitrative tumour growth with migration-proliferation dichotomy. *Math. Modelling Natur. Phenom.* **6–7** (2011), 27–38.

13. R. Roe-Dale, D. Isaacson, and M. Kupferschmid, A mathematical model of breast cancer treatment with CMF and Doxorubicin. *Bulletin Math. Biology* **73-3** (2011), 585–608.

14. M. D. Smith, A. D. Smirthwaite, D. E. Cairns, R. B. Cousins, and J. D. Gaylor, Techniques for measurement of oxygen consumption rates of hepatocytes during attachment and post-attachment. *Inte. J. Artif. Organs* **19-1** (1996), 36–44.

15. W. Y. Tan and L. Hanin, *Handbook of Cancer Models and Applications*. World Scientific Publishing, New Jersey, 2008.

16. A. Tovar, N. M. Patel, G. L. Niebur, M. Sen, and J. E. Renaud, Topology otimization using a hybrid cellular automaton method with local control rules. *J. Mech. Design* **128-6** (2006), 1205–1216.